

Synthesis and characterization of asphalt composite precursors using amorphous rice husk silica

(Síntese e caracterização de precursores de compósitos asfálticos utilizando sílica de casca de arroz amorfa)

S. Sembiring^{1*}, R. Situmeang², Z. Sembiring²

¹Lampung University, FMIPA, Department of Physics, Jl. Prof. Soemantri Brojonegoro No. 1 Bandar Lampung, 35145, Indonesia

²Lampung University, FMIPA, Department of Chemistry, Indonesia

Abstract

In this research, asphalt composites were produced by mixing asphalt with silica extracted from rice husk, with a ratio of asphalt to silica of 1:0, 1:1.7 and 1:2, and calcined at 150 °C. Development of structures was characterized using Fourier transform infrared (FTIR) spectroscopy, X-ray diffraction (XRD), scanning electron microscopy (SEM), followed by differential thermal analysis (DTA/TGA). The FTIR results showed the presence of Si-OH, C=O, and C-H functional groups, which were associated with asphaltene, carbon, and silica, according to the XRD analysis. The results obtained also indicated the significant effect of rice husk silica addition on phase transformation of asphaltene into silica and carbon, while asphaltene molecules were practically undetected. The presence of silica and carbon resulted in increased decomposition temperature of the sample. Based on these characteristics, the samples were considered as a roof material, suggesting their potential use as a substitute for lightweight steel roof devices.

Keywords: rice husk, silica, asphalt, structure, thermal behavior.

Resumo

Nesta pesquisa, compósitos asfálticos foram produzidos misturando asfalto com sílica extraída da casca de arroz, com relação asfalto:sílica de 1:0, 1:1,7 e 1:2, e calcinados a 150 °C. O desenvolvimento das estruturas foi caracterizado por espectroscopia no infravermelho com transformada de Fourier (FTIR), difração de raios X (XRD), microscopia eletrônica de varredura, seguida de análise térmica diferencial. Os resultados de FTIR mostraram a presença dos grupos funcionais Si-OH, C=O e C-H, que foram associados ao asfalto, carbono e sílica, de acordo com a análise de DRX. Os resultados obtidos também indicaram o efeito significativo da adição de sílica de casca de arroz na transformação de fase do asfalto em sílica e carbono, enquanto as moléculas de asfalto praticamente não foram detectadas. A presença de sílica e carbono resultou em aumento da temperatura de decomposição da amostra. Com base nessas características, as amostras são consideradas como material para uso em telhado, sugerindo seu uso potencial como substituto para dispositivos de teto de aço leve.


Palavras-chave: casca de arroz, sílica, asfalto, estrutura, comportamento térmico.

INTRODUCTION

Asphalt is a by-product of the distillation process of crude oil and is composed of various hydrocarbons consisting primarily of molecules that contain mainly carbon and hydrogen atoms. Asphalt has a complex chemical composition which exhibits complex physical properties such as viscous and elastic behaviors [1]. For example, cohesion and viscosity of asphalt may increase with the addition of other particles, which are good at high temperature [2]. Besides that, asphalt can exist as a fluid of low viscosity at high temperatures and as a very brittle material at low temperatures [1]. One of the inorganic additives that have

been used intensively is silica to improve the properties of asphalt. Silica has also gained great attention by researchers for preparing asphaltic materials with desirable properties because of its excellent stability, high surface area, chemical purity, strong adsorption, and good dispersing ability [3-5]. For example, silica has been used to reinforce cementitious mixtures [6] and elastomers [7]. In a study [8], the asphalt binder was modified with silica at contents of 4 and 6 wt%. It has been observed that the performances of aging, rutting, and fatigue cracking of silica-modified binders have been improved. The use of nanoclays as asphalt modifiers is due to their abundance in nature, low cost of production, and small amounts needed for asphalt modification [9]. Jahromi and Khodaii [10] have investigated the effect montmorillonite-based nanoclays on physical properties of asphalt. They found that the addition of nanoclays improves

*simonsembiring2@gmail.com

 <https://orcid.org/0000-0002-6499-0598>

the temperature susceptibility of asphalt and its aging resistance. As the silica material is highly reactant with the asphalt binder than conventional fillers, with good dispersal ability of silica particles into asphalt binder, one can prepare polymeric nanocomposite with desirable performance [11, 12].

Many researchers have investigated the potential of rice husk as an excellent source of high-grade amorphous silica, which can be extracted by relatively simple methods [13-15]. Due to the high surface area, high degree of amorphization, and fine particle size, rice husk silica has been shown to be a good material for the preparation and synthesis of various materials such as the production of nanosilica [16, 17], borosilicate [18], carbosil [19], aluminosilicates [20], mullite [21], cordierite [22], and forsterite [23]. Taking advantage of rice husk silica characteristics, the main objective of this study is an exploration of rice husk silica to provide some insight into choosing the basic materials in design and preparation of asphalt composite for roof materials as a substitute for lightweight steel roof with a variation of silica. To gain insight on several basic characteristics, the samples were studied using various techniques include FTIR for functionality, XRD for structure, SEM for microstructure, and DTA/TGA for thermal analysis.

EXPERIMENTAL PROCEDURE

Materials: the silica feedstock was taken from rice husk obtained from the local rice milling industry. The reagent grade chemicals used were 5% NaOH 5%, 5% HCl (purity ~99.0%), and absolute alcohol (C₂H₅OH) purchased from Merck kGaA (Darmstadt, Germany), and distilled water. An asphalt obtained from Buton refinery, Southeast Sulawesi Province, Indonesia, was used in the present investigation.

Preparation of asphalt composite: rice husk silica was produced using alkali extraction method following the procedure reported in a previous study [23]. In this stage, 50 g dried husk was mixed with 500 mL of 5% KOH solution in a beaker glass, boiled for 30 min, and followed to cool to room temperature and left for 24 h. The mixture was filtered to separate the filtrate which contained silica sol. The sol obtained was acidified by dropwise addition of 5% HCl solution until the conversion of the sol into gel was completed. The gel was oven dried at 110 °C for 8 h and then ground into powder by mortar and sieved to obtain the powder with the size of 200 mesh. For the preparation of asphalt composite precursor, 50 g of asphalt was heated to 100 °C and blended with silica from rice husk using a shear mixer at a rate of 125 rpm for 3 h. Rice husk silica was blended with the asphalt at different ratio of asphalt to silica (1:0, 1:1.7 and 1:2) to determine the effect of silica on the structural properties of asphalt composite. The samples were pressed in a metal die with the pressure of 2×10^4 N/m² to produce a cylindrical pellet and then the pellets were calcined at 150 °C for 6 h.

Characterization: the infrared spectra were recorded using a Perkin Elmer FTIR (Fourier transform infrared)

spectrometer by scanning in wavenumbers ranging from 4000-400 cm⁻¹. X-ray diffraction (XRD) analyses were conducted by employing an automated Shimadzu XD-610 diffractometer equipped with an FK 60-04 air insulated XRD tube. The XRD patterns were taken with CuK α radiation ($\lambda=1.5406$ nm) at 40 kV and 30 mA in the range of $2\theta=5^\circ-100^\circ$, with a step size of 0.02° , counting time 1 s/step and 0.15° receiving slit. Polished and thermally etched samples were used for microstructural analysis conducted with a scanning electron microscope, SEM Philips-XL. Thermal analysis was performed using DTA Merck Setaram Tag 24 S, under a nitrogen atmosphere with a constant heating rate of 3 °C/min. The thermogram was produced by scanning the sample between 30 to 800 °C.

RESULTS AND DISCUSSION

Functional characteristics of asphalt composite: to compare the functionality of the asphalt with different silica addition, the samples were characterized using FTIR spectroscopy. Fig. 1a shows the spectrum of the asphalt without silica sample and Figs. 1b and 1c present the spectra of the samples with different ratios of asphalt to silica. The spectrum of the asphalt without silica sample (Fig. 1a) was characterized by the existence of several absorption bands associated with asphalt commonly reported in the literature [24-28]. The most obvious peak was located at around 1752 cm⁻¹, which is commonly assigned to stretching vibration of carbonyl C=O group (i.e., carboxylates, ketones, and/or anhydrides). The peaks at 958, 816 and 749 cm⁻¹ were related to the bending vibrations of C-H in phenyl. Others strong bands were located at 2938 and 1474 cm⁻¹, which were probably the characteristics stretching vibrations of O-H from carboxylic acids and C-H from alkanes. Figs. 1b and 1c indicate the significant effect of silica addition on the functionality of the samples. The most obvious change is the presence of peaks associated with silica hydroxide, confirming the presence of water molecules during the blending process. As shown in Figs. 1b and 1c, a peak was located at around 3709 cm⁻¹, which is commonly assigned to stretching vibration of O-H bond. This absorption band most likely arises from the O-H bond of silanol group in Si(OH)₄ and water molecule [29], as a result of bending vibration of the H-OH. The presence of Si(OH)₄ is supported by the existence of absorption band at 1102 cm⁻¹, which is commonly assigned to stretching vibration of Si-O-Si due to the deformation of Si-O bond, as was observed in [30, 31]. The presence of absorption peak at 1102 cm⁻¹ suggested that the sample was still dominated by Si(OH)₄. The results for the samples with the addition of silica (Figs. 1b and 1c) also displayed a gradual disappearance of absorption peaks at 1752 cm⁻¹. This implied the decomposition of Si(OH)₄ with the release of carbonyl C=O species, which also suggested that the complete transformation of Si(OH)₄ into oxide was achieved at this condition. In addition, the intensity of the band assigned to O-H bonds increased to form Si(OH)₄ molecules. However, the addition of silica seemed to

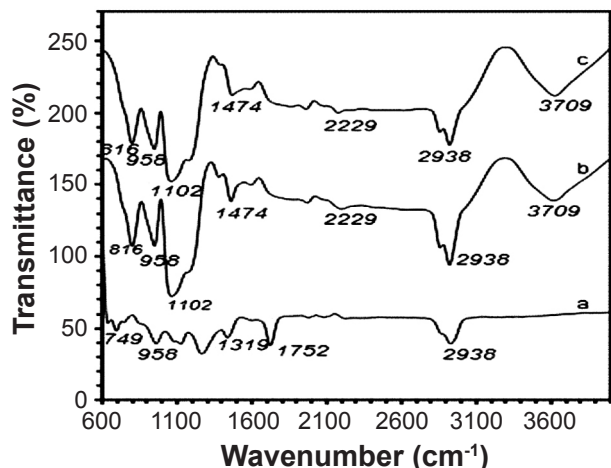


Figure 1: FTIR spectra of the samples with different ratios of asphalt to silica: a) asphalt without silica; b) 1:1.7; and c) 1:2. [Figura 1: Espectro de FTIR das amostras com diferentes relações asfalto:silica: a) asfalto sem silica; b) 1:1,7; e c) 1:2.]

influence the intensity of the chemical groups of the asphalt; therefore, it affected the overall performance of the material. Thus, it was concluded that the asphalt exhibited a change in its interbond with the addition of silica.

Structural characteristics of asphalt composite: characterization of the samples using the XRD technique was conducted to evaluate the crystallographic structure of the sample. The XRD patterns of the samples are shown in Fig. 2. Fig. 2a shows the pattern of the sample without silica addition and Figs. 2b and 2c present the pattern of the samples with different ratios of asphalt to silica. The wide peaks at 18° – 26° and 42° in Fig. 2a represent the XRD pattern of asphalt without silica. A peak appeared around $2\theta=18.7^{\circ}$ because of the aliphatic chain or thick saturated rings. The peak settled at approximately $2\theta=23.5^{\circ}$ is known as the multilayered graphene, not at the $2\theta \sim 26^{\circ}$ observed in the literature [32], probably due to the weak bond between the carbon layers. The multilayered graphene is produced by stacking aromatic molecules in the asphalt reaction process [33]. The presence of graphene was also supported by a weak peak at $2\theta=42.25^{\circ}$, which is due to the influence of asphaltene in the nearest neighbors in the ring structure, as

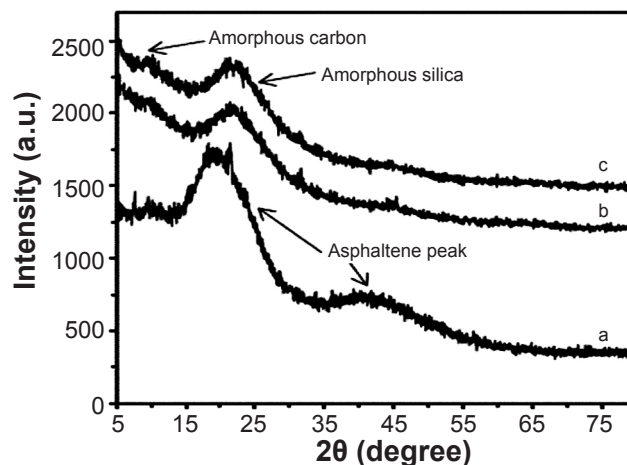


Figure 2: X-ray diffraction patterns of samples with different ratios of asphalt to silica: a) asphalt without silica; b) 1:1.7; and c) 1:2. [Figura 2: Difractogramas de raios X das amostras com diferentes relações asfalto:silica: a) asfalto sem silica; b) 1:1,7; e c) 1:2.]

supported by previous studies [34, 35]. The XRD pattern of the sample without silica addition (Fig. 2a) showed quite different characteristics to those observed for the other two samples (Figs. 2b and 2c). As displayed by these patterns, the phases of the samples were marked by the existence of a broad peak located at around $2\theta=22^{\circ}$, suggesting that the silica was amorphous, with amorphous carbon at $2\theta=5$ – 10° .

Microstructural characteristics of asphalt composite: the surface morphologies of the samples at different silica addition were characterized using SEM. The micrographs presented in Fig. 3 demonstrate the effect of silica addition on the size and distribution of the silica particles and asphalt matrix on the surface. The surface morphologies of the samples were marked by the existence of particles with different grain sizes and distributions. The microstructure of the sample without silica (Fig. 3a) revealed quite different characteristics to those observed for the other two samples (Figs. 3b and 3c). In addition, it was obvious that the clusters in the sample without silica were surrounded by large grains. The large clusters were most likely composed of asphaltene structure. The surfaces of samples with silica addition (Figs. 3b and 3c) were dominated by smaller grains

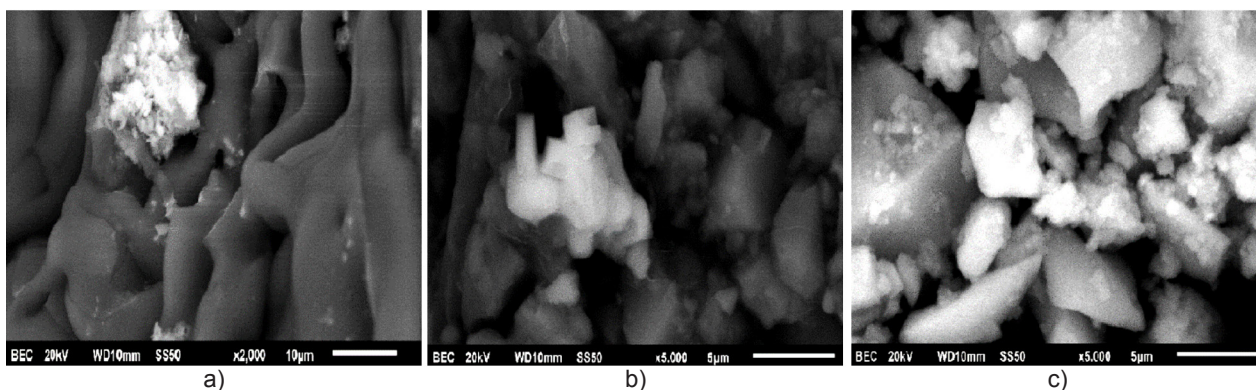


Figure 3: Scanning electron microscopy (SEM) images of the samples with different ratios of asphalt to silica: a) asphalt without silica; b) 1:1.7; and c) 1:2.

[Figura 3: Imagens de MEV das amostras com diferentes relações asfalto:silica: a) asfalto sem silica; b) 1:1,7; e c) 1:2.]

Table I - Composition of samples (wt%) according to EDS analysis.

[Tabela I - Composição das amostras (% em massa) de acordo com a análise de EDS.]

Sample	Carbon	Na ₂ O	SiO ₂	SO ₃	Cl
Asphalt	91.8	-	-	8.2	-
1:1.7	63.3	3.1	29.0	3.0	1.6
1:2	53.2	1.2	41.7	3.6	0.3

composed of silica clusters and covered with some large grains of asphaltene structure. Due to the agglomeration of silica, the silica group reacted with the asphalt binder, and the size of the silica group became smaller. Both samples were marked by initiation as a result of silica crystallization. This feature suggested that at the ratios 1:1.7 and 1:2, the silica phase continued to change and allowed the particle arrangement, leading to initiation of the formation of asphalt-silica composite. This change was supported by the result of XRD analysis (Figs. 2b and 2c) and EDS (energy dispersive spectroscopy) analysis (Table I), in which silica was detected. By comparing the contents of the elements in the asphalt-silica composites, according to the values of C (63.3%) and SiO₂ (29.0%) for 1:1.7 ratio, and C (53.2%) and SiO₂ (41.7%) for 1:2 ratio, it can be seen that some difference should be addressed. This difference was most likely due to the formation of carbon (C) and silica (SiO₂), as observed using the XRD method (Fig. 2). The presence of impurities was indicated by the FTIR results previously presented (Fig. 1 and Table I).

Thermal characteristics of asphalt composite: in this study, thermal characteristics of the samples were determined by analyzing the samples with thermal gravimetric analysis (TGA) and differential thermal analysis (DTA). The TGA thermograms of the samples with different silica addition are depicted in Fig. 4 and the corresponding DTA results are presented in Fig. 5. The TGA results indicated the existence of three temperature zones, indicating the pattern of weight loss of the samples. At temperature range up to 230 °C, for all samples the weight loss was very small, showing the endothermic peak associated with the removal of water and volatile components of the asphalt compound. At the range from 230 to 471 °C, the results indicated very sharp weight loss. This part of the thermogram indicated very evidently the ingredients decomposition of the asphalt compound and crystallization of silica which was supported by the existence of an exothermic peak at 471 °C in the DTA thermograms in Fig. 5. Above 471 °C, the samples practically reached a stable state, since no more weight loss was displayed by the samples (Fig. 4). As shown in Fig. 5a, the asphalt without silica sample showed the existence of two endothermic peaks at around 76 and 420 °C, and one exothermic peak at around 471 °C. The peak at 76 °C was most likely due to the evaporation of water and residual organics probably present during the preparation of the sample. The peaks at around 420 and 471 °C could be assigned to the dehydration

of asphaltene molecules, as supported by XRD results (Fig 2a). In the samples with silica addition (Figs. 5b and 5c), it can be seen that the peak associated with evaporation of water was much smaller compared to that observed in the sample in Fig. 5a, suggesting that samples contained less water and were denser. In addition, it was quite evident that phase transformation took place as indicated by an increased peak at 471 °C, indicating that carbon and silica have been produced, as supported by XRD results and observed by others [36]. This means that silica particles and asphalt chain mixed homogeneously to form a more compact structure. Comparing the data for the sample asphalt without silica to those for the samples filled with silica (Table II), it can be seen that the effect of the amount of silica added was practically similar. The main difference observed was considerably lower decomposition temperature and less compact structure of the asphalt without silica sample than those observed for the samples with silica addition (Table II). The main reason

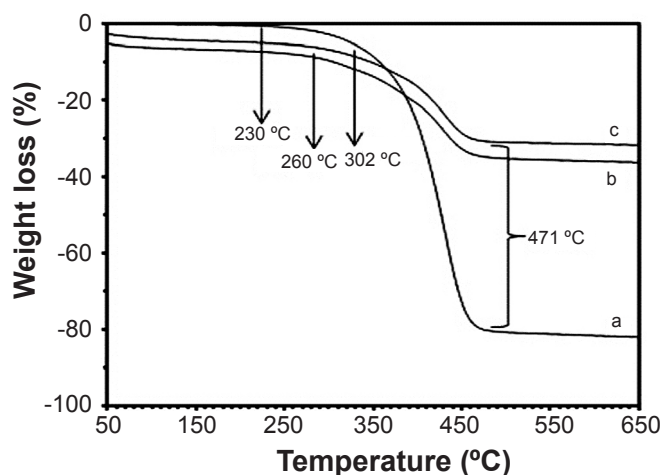


Figure 4: TGA thermograms of the samples with different ratios of asphalt to silica: a) asphalt without silica; b) 1:1.7; and c) 1:2. [Figura 4: Termogramas de ATG das amostras com diferentes relações asfalto:silica: a) asfalto sem silica; b) 1:1,7; e c) 1:2.]

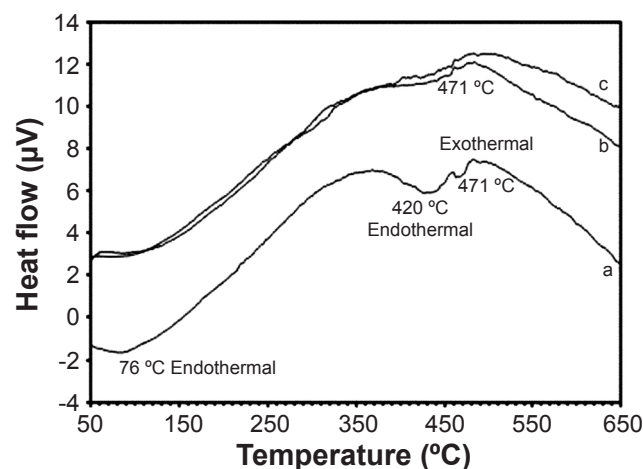


Figure 5: DTA thermograms of the samples with different ratios of asphalt to silica: a) asphalt without silica; b) 1:1.7; and c) 1:2. [Figura 5: Termogramas de ATD das amostras com diferentes relações asfalto:silica: a) asfalto sem silica; b) 1:1,7; e c) 1:2.]

Table II - Summary of TGA results for all samples.

[Tabela II - Resumo dos resultados de ATG de todas as amostras.]

Sample	Onset temp. (°C)	Max. temp. (°C)	Weight loss, 30-300 °C (%)	Weight loss, 300-500 °C (%)	Mass residue >500 °C (%)
Asphalt	230	453	0.5	79.9	19.6
1:1.7	260	471	8.2	34.9	56.9
1:2	302	497	5.9	29.6	64.5

for this difference is most likely the higher crystallinity of the sample with silica addition, as a result of silica added, as supported by the results of the XRD analysis (Fig. 2). Higher crystallinity of silica promoted thermal stability of the composite, leading to higher decomposition temperature as shown in Table II.

CONCLUSIONS

From a series of experiments conducted in this study, some conclusions were obtained regarding the effects of adding different ratios of asphalt to silica on structural properties of asphalt composite. FTIR results indicated the presence of Si-OH, C=O, and C-H functional groups, which were associated with silica and carbon from the reaction between asphaltenes and silica as verified by XRD analysis. In addition, phase transformation was found to result in the change of the characteristics of the asphaltenes related to silica and carbon formation, including increased decomposition temperature and compaction of the asphalt with the addition of silica sample. Based on these characteristics, the samples were considered as a roof material, suggesting their potential use as a substitute for lightweight steel roof devices.

ACKNOWLEDGMENT

The authors wish to thank and appreciate Ministry of Research, Technology, and High Education, Directorate General of Strengthening Research and Development, Republic of Indonesia for research funding provided through Hibah Competence Research Grant Batch I No: 062/SP2H/LT/DRPM/2018 Program in 2018.

REFERENCES

[1] J.F. Branthaver, J.C. Petersen, R.E. Robertson, J.J. Duvall, S. Kim, "Binder characterization and evaluation", **2**, Nat. Res. Council, Washington (1993).
 [2] L. Ping, L. Yunlong, *Appl. Mech. Mater.* **587** (2014) 1220.
 [3] L. Senff, J.A. Labrincha, V.M. Ferreira, D. Hotza, W.L. Repette, *Constr. Build. Mater.* **23**, 7 (2009) 2487.
 [4] D. Kong, X. Du, S. Wei, H. Zhang, Y. Yang, S.P. Shah, *Constr. Build. Mater.* **37** (2012) 707.
 [5] L.P. Singh, S.R. Karade, S.K. Bhattacharyya, M.M. Yousuf, S. Ahalawat, *Constr. Build. Mater.* **47** (2013) 1069.
 [6] G. Quercia, H.J.H. Brouwers, in 8th fib PhD Symp. Civil Eng., Denmark (2010).

[7] K. Chrissafis, K.M. Paraskevopoulos, G.Z. Papageorgiou, D.N. Bikiaris, *Appl. Polym. Sci.* **110** (2008) 1739.
 [8] H. Yao, Z. You, L. Li, C.H. Lee, D. Wingard, Y.K. Yap, X. Shi, S.W. Goh, *Mater. Civ. Eng.* **25**, 11 (2012) 1619.
 [9] H.Y. Yu, X. Zeng, S.P. Wu, L. Wang, G. Liu, *Mater. Sci. Eng. A* **447**, 1-2 (2007) 233.
 [10] S.G. Jahromi, A. Khodaii, *Constr. Build. Mater.* **23**, 8 (2009) 2894.
 [11] P.C. LeBaron, Z. Wang, T.J. Pinnavaia, *Appl. Clay. Sci.* **15**, 1-2 (1999) 11.
 [12] S.S. Ray, M. Okamoto, *Prog. Polym. Sci.* **28**, 11 (2003) 1539.
 [13] M.M. Haslinawati, K.A.Z. Matori, Z.A. Wahab, H.A.A. Sidek, A.T. Zainal, *Int. Basic Appl. Sci.* **9**, 9 (2009) 22.
 [14] E. Rafiee, S. Shahebrahimi, M. Feyzi, M. Shaterzadeh, *Int. Nano Lett.* **2**, 29 (2012) 1.
 [15] B.I. Ugheoke, O. Mamat, *Inter. Mater. Eng. Innov.* **3**, 2 (2012) 139.
 [16] K. Amutha, R. Ravibaskar, G. Sivakumar, *Int. J. Nanotechnol. Appl.* **4**, 1 (2010) 61.
 [17] T.H. Liou, C.C. Yang, *Mat. Sci. Eng. B* **176** (2011) 521.
 [18] S. Sembiring, *Indo. Chem.* **11**, 1 (2011) 85.
 [19] W. Simanjuntak, S. Sembiring, K. Sebayang, *Indo. Chem.* **12**, 1 (2012) 119.
 [20] W. Simanjuntak, S. Sembiring, P. Manurung, R. Situmeang, I.M. Low, *Ceram. Int.* **39**, 8 (2013) 9369.
 [21] S. Sembiring, W. Simanjuntak, P. Manurung, D. Asmi, I.M. Low, *Ceram. Int.* **40**, 5 (2014) 7067.
 [22] S. Sembiring, W. Simanjuntak, R. Situmeang, A. Riyanto, K. Sebayang, *Ceram. Int.* **42**, 7 (2016) 8431.
 [23] S. Sembiring, A. Riyanto, W. Simanjuntak, R. Situmeang, *Orient. Chem.* **33**, 4 (2017) 186.
 [24] F. Zhang, J. Yu, J. Han, *Constr. Build. Mater.* **25** (2011) 129.
 [25] C. Fang, R. Yu, Y. Li, M. Zhang, J. Hu, M. Zhang, *Polym. Test.* **32**, 5 (2013) 953.
 [26] A.R. Abbas, U.A. Mannan, S. Dessouky, *Constr. Build. Mater.* **45** (2013) 162.
 [27] G. Socrates, *Infrared and Raman characteristic group frequencies: tables and charts*, 3rd Ed., Wiley (2001).
 [28] J.F. Masson, L. Pelletier, P. Collins, *Appl. Polym. Sci.* **79**, 6 (2001) 1034.
 [29] F. Adam, J.H. Chua, *J. Colloid Interface Sci.* **280**, 1 (2004) 55.
 [30] M.T. Tsai, *J. Eur. Ceram. Soc.* **22** (2002) 1085.
 [31] T. Jiang, Q. Zhao, H. Yin, *Appl. Clay. Sci.* **35** (2007) 155.
 [32] T.H. Dunning, *J. Chem. Phys.* **90** (1989) 1023.

[33] I.F. Cheng, Y.R. Xie, R.A. Gonzales, P.R. Brejna, J.P. Sundararajan, B.A.F. Kengne, D.E. Aston, D.N. McIlroy, J.D. Foutch, P.R. Griffiths, *Carbon* **49** (2011) 2852.

[34] V.S. Babu, L. Farinash, M.S. Seehra, *J. Mater. Res.* **10** (1995) 1075.

[35] V.S. Babu, M.S. Seehra, *Carbon* **34** (1996) 1259.

[36] C.H. Xu, Y.Z. Lin, J.M. Xiang, Q.H. Wang, *China Synth. Rubber Indus.* **8** (1985) 419.

(*Rec.* 27/04/2018, *Rev.* 12/07/2018, 07/10/2018, 12/11/2018, *Ac.* 12/11/2018)

